molecular pharmaceutics

Article

pubs.acs.org/molecularpharmaceutics

Preclinical Evaluation of DO3A-Act-AQ: A Polyazamacrocyclic Monomeric Anthraquinone Derivative as a Theranostic Agent

Anupriya Adhikari,[†,‡] Anupama Datta,[*,†] Manish Adhikari,[§] Kanchan Chauhan,[†] Krishna Chuttani,[†] Sanjiv Saw,[⊥] Abha Shukla,[‡] and Anil K. Mishra[*,†]

[†]Division of Cyclotron and Radiopharmaceutical Sciences, Institute of Nuclear Medicine and Allied Sciences, Defence Research & Development Organization, Brig S K Mazumdar Road, Delhi-110054, India

[‡]Department of Chemistry, Kanya Gurukul Campus, Gurukul Kangri Vishwavidyalaya, Haridwar-249404, India

[§]Division of Radiation Biosciences, Institute of Nuclear Medicine and Allied Sciences, Defence Research & Development Organization, Brig S K Mazumdar Road, Delhi-110054, India

[⊥]Division of Clinical PET, Institute of Nuclear Medicine and Allied Sciences, Defence Research & Development Organization, Brig S K Mazumdar Road, Delhi-110054, India

Supporting Information

ABSTRACT: An anthraquinone conjugated macrocyclic chelating agent, 2,2′,2″-(10-(2-(9,10-dioxo-9,10-dihydroanthracen-1-ylamino)-2-oxoethyl)-1,4,7,10-tetraazacyclododecane-1,4,7-triyl)triacetic acid or DO3A-Act-AQ, was synthesized by reacting trisubstituted cyclen (DO3A) with 2-chloro-*N*-(9,10-dioxo-9,10-dihydro-anthracen-1-yl)-acetamide and radiolabeled with $^{68}GaCl_3$ in 84% efficiency and a specific activity of 4.62 MBq/nmol. The IC_{50} value for BMG-1 cells was 0.1 mM, while the same concentration of DO3A-Act-AQ rendered no significant toxicity in HEK cells. The exposure of BMG-1 cells with 0.1 mM DO3A-Act-AQ displayed a time-dependent increase in apoptosis (40.7% at 4 h and 53% at 24 h), and the effect was 2.8- and 3.6-fold % higher as seen in HEK cells. An increase in S-phase cell population suggested S-phase arrest concomitant with induction of apoptosis in BMG-1 cells reaching to 4.5 times after 24 h with respect to control cells. DNA binding studies on CT-DNA (calf thymus) revealed a quenching pattern in the presence of DO3A-Act-AQ (10−70 μM), and the Stern−Volmer quenching constant was 2.4157×10^6 L mol^{-1}, indicative of strong binding with ds-DNA. A decrease in the positive and negative bands of CT-DNA was seen at 278 nm and 240 nm, respectively, on addition of 0.05 mM of DO3A-Act-AQ in CD studies. ^{68}Ga-DO3A-Act-AQ was stable *in vitro* in both PBS and human serum for at least 2 h. The *in vivo* blood kinetics study performed on normal rabbits indicated fast clearance with $t_{1/2}(F) = 40 \pm 0.3$ min and $t_{1/2}(S) = 3$ h 30 min $\pm$ 0.1 min. *Ex vivo* biodistribution analysis displayed a favorable tumor-to-muscle ratio of 8.4 after 2 h in athymic nude mice xenografted with BMG-1 cells, suggesting the specificity of ^{68}Ga-DO3A-Act-AQ toward tumors.

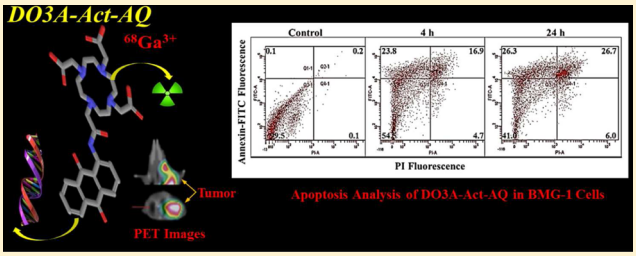

KEYWORDS: *anthraquinone, CT-DNA, BMG-1, HEK, gallium-68, PET, cancer*

INTRODUCTION

Despite phenomenal advances in the understanding of the diseases, cancer still remains the leading cause of death worldwide. Therefore, new strategies for combined diagnostic and therapeutic are imperative for the early diagnosis of cancer and appropriate therapeutic strategy.[1] In addition to the surgical removal of tumor tissue, other modes of pretreatment include chemotherapy, radiotherapy, and immunotherapy. Currently, a wide range of chemotherapeutic agents in the form of alkylating agents, DNA intercalator, and antimetabolites are known wherein they affect cell division or DNA synthesis, leading to inhibition of cell growth and cell death. There is a continuing interest in the development of new agents in which the anthraquinone base structure represents an attractive target for the design of new anticancer agent due to its strong role in the control of cell proliferation. Anthraquinone, having a planar tricyclic structure, is the backbone of many known antitumor drugs like doxorubicin and mitoxantrone capable of targeting at the molecular/DNA level.[2] They are known for their foremost property of intercalation between the DNA base pairs, causing an unwinding of the helix leading to miscoding and possible cell apoptosis.[3] Gadolinium complexes of 1,4- and 1,5-diaminoanthraquinone conjugated 1,4,7,10-tetraazacyclododecane-1,4,7,10-tetraacetic acid (DOTA) based compounds are reported to bind with the specific DNA sequence open-d(ATCGAGACGTCTCGAT)$_2$.[4] Recently, mono- and dime-

Received: July 16, 2013
Revised: December 17, 2013
Accepted: December 22, 2013
Published: December 23, 2013

tallic Au(I) triphenylphosphine complexes derived from 1,2-, 1,4-, and 1,8-dialkynyloxyanthraquinone have been synthesized, and their cytotoxicities on the cancer cell line (MCF-7) and fluorescence cell imaging have been reported.[5] 1,4- and 1,8-Bis-substituted anthracenedione derivatives inhibit the activity of telomerase.[6] Aminoacylhydroxyanthraquinone bearing glycyl, valyl, lysyl, and tryptophanyl residues, 1,4-bis(2-aminoethylamino)anthraquinone−amino acid conjugates, and 1,4-diamidoanthraquinone derivatives were reported to exhibit significant DNA binding (intercalation) or cytostatic or cytotoxic activities in cancer cells.[7−15]

In nuclear imaging, the use of stable complexes with radiometals is a crucial factor for the development of metal-based imaging and therapeutic agents. The lanthanide (trivalent) complexes of polyazapolycarboxylic macrocycle with seven to eight donor atoms such as with DOTA are known for their strong complexation stability, unusually rigid, highly symmetrical structure, and adopting the same geometry in solution as well as the solid state in comparison with noncyclic ligands such as DTPA, even though both are octadentate chelate. Positron emission tomography (PET) is a renowned imaging modality, and recently worldwide interest in ^{68}Ga as a radioisotope for PET which gives high-resolution images of the functional processes in the body has enhanced rapidly because of its appropriate properties for high-quality PET imaging.[16−18]

The anthraquinone moiety has been much explored for cellular/*in vitro* imaging, but *in vivo* studies using ^{68}Ga have not yet been exploited in detail. This prompted us to work with anthraquinone and to determine its potential as a therapeutic and PET imaging probe. The current work has been directed toward the development of an imaging as well as therapeutic agent. The potential of the ligand as a tumor-specific agent was evaluated after its synthesis and radiolabeling with ^{68}Ga. Here, we report the synthesis of a macrocyclic ligand conjugated with DNA binding ligand anthraquinone (DO3A-Act-AQ) showing specificity to the tumor using PET imaging and biodistribution performed on athymic nude mice xenografted with BMG-1 cells. DNA (calf thymus) binding studies were also performed using fluorescence and circular dichroism (CD) spectroscopic techniques. The therapeutic potential of the synthesized macrocyclic derivative was assessed by determining the protonation constant and complexation behavior of DO3A-Act-AQ with therapeutic metals like Sm(III) and Lu(III). The cytotoxicity, induction of apoptosis, and effect on cell cycle in both cancer and normal cells were assessed by MTT assay and flow cytometric methods, respectively, to further evaluate its therapeutic behavior.

MATERIALS AND METHODS

Chemicals. 1,4,7,10-Tetraazacyclododecane was purchased from Strem, France. 1-Aminoanthraquinone, *tert*-butylbromoacetate, 2-chloroacetylchloride, potassium carbonate, potassium iodide, *N*,*N*-diisopropylethylamine (DIPEA), pyridine, dry acetonitrile, methanol, dichloromethane, toluene, trifluoroacetic acid, water, chloroform, and ethanol were purchased from Sigma-Aldrich, USA. Column chromatography was carried out using silica MN60 (60−200 μm). Thin layer chromatography (TLC) was checked on aluminum plates coated with silica gel 1160, F_{254} (Merck, Germany), and visualized under UV light 254 nm. For the potentiometric studies, the chemicals used were of the highest analytical grade. The metal salts, $SmCl_3 \cdot 6H_2O$, $LuCl_3 \cdot 6H_2O$, $CuSO_4 \cdot 5H_2O$, and $Ga(NO_3)_2 \cdot xH_2O$ were purchased from Aldrich (99.9%). Stock solutions of the individual metal cations were prepared by dissolving respective metal salts in water, and their concentration was determined by complexometric titration with standardized Na_2H_2-EDTA (ethylenediaminetetraacetic acid) and xylenol orange as an indicator. Radiocomplexation and the radiochemical purity was checked by instant thin layer chromatography (ITLC-SG) strips and radio-TLC. High glucose Dulbecco's modified Eagle's medium (HG-DMEM), trypsin-EDTA, bovine serum albumin (BSA), Hank's balanced salt solution (HBSS), crystal violet, propidium iodide (PI), annexin V−PI kit, RNase A and low melting agarose (LMA), and ethidium bromide (EB) were obtained from Sigma-Aldrich, St. Louis, MO, USA. Phosphate-buffered saline (PBS), 3-(4,5-dimethylthiazol-2-yl)-2,5-diphenyltetrazolium bromide (MTT), and citric acid were procured from Himedia Laboratory Pvt. Ltd., Mumbai, India.

Instrumentation. ^{1}H and ^{13}C NMR spectra were recorded on a Bruker Avance II 400 MHz (Switzerland). High-resolution electrospray-ionization mass spectrometry (ESI-MS) was carried out on Bruker micrOTOF-Q II and Agilent 6540 UHD accurate mass Q-TOF LC/MS. HPLC analyses were performed on Agilent 1200 LC coupled to a UV detector (λ = 214 and 254 nm). The C-18 RP Agilent columns (5 μm, 4.6 mm × 250 mm, 5 μm, 9.4 mm × 250 mm) and mobile phase (System A: 20% methanol and 80% water; System B: 10% acetonitrile and 90% water) were used. The flow rate for analytical HPLC was 0.5 mL/min, while that for preparative HPLC was 10 mL/min. Flow cytometric measurements were carried out using a FACS calibur flow cytometer (Becton Dickinson and Co., Franklin Lakes, NJ, USA). Radiolabeling studies and potentiometric measurements were carried out using a γ-scintillation counter GRS230, ECIL (India) and an automatic titration system consisting of Metrohm 713 pH meter equipped with a Metrohm A.60262.100 electrode and 800 Dosino autoburet, respectively. CD spectra were measured on a JASCO 815 spectrophotometer, and the MTT assay absorbance was read at 570 nm using 630 nm as a reference wavelength on an ELISA reader (BioTek instruments, Vinooski, VT, USA). PET imaging was performed using a Discovery STE 16 (GE) system. UV−vis and fluorescence studies were performed in a Biotek synergy H4 hybrid multiplate reader.

Synthetic Approach. *tert-Butyl-2,2′,2″-(1,4,7,10-tetraazacyclododecane-1,4,7-triyl)triacetate (**1**).* Synthesis was performed as reported in the literature (see also Scheme 1).[19] Briefly, to a stirring solution of 1,4,7,10-tetraazacyclododecane (1.5 g, 8.72 mmol) in dry acetonitrile (100 mL) was added $NaHCO_3$ (2.19 g, 26.0 mmol) at 0 °C. This was followed by the dropwise addition of *tert*-butyl bromoacetate (3.86 mL, 26.0 mmol). The reaction was further allowed to reach 25 °C and stirred for 48 h. After 48 h the reaction mixture was filtered, and the filtrate was evaporated under pressure to obtain the crude product. It was purified by open column chromatography on silica gel, R_f = 0.7 (eluent: $CHCl_3$/CH_3OH: 9.5/0.5) to give the desired product as a white solid in 80% yield (3.5 g). The final product was well-characterized by ^{1}H, ^{13}C NMR, and mass spectrometry. ^{1}H NMR ($CDCl_3$, 400 MHz): δ_H = 3.18−3.28 (s, 6H, CH_2), 2.89−2.94 (m, 16H, CH_2), 1.437 (s, 27H, CH_3) ppm; ^{13}C NMR ($CDCl_3$, 100 MHz): δ_C = 170.52, 169.63, 81.94, 81.69, 58.22, 51.36, 51.24, 49.21, 48.79, 47.52, 28.24, 28.20 ppm; HR-ESI-MS calculated for $[C_{26}H_{50}N_4O_6 + Na]^+$: 537.3628; found $[M + Na]^+$: 537.3631.

dx.doi.org/10.1021/mp4004089 | *Mol. Pharmaceutics* 2014, 11, 445−456

Scheme 1. Representation for the Synthesis of DO3A-Act-AQ[a]

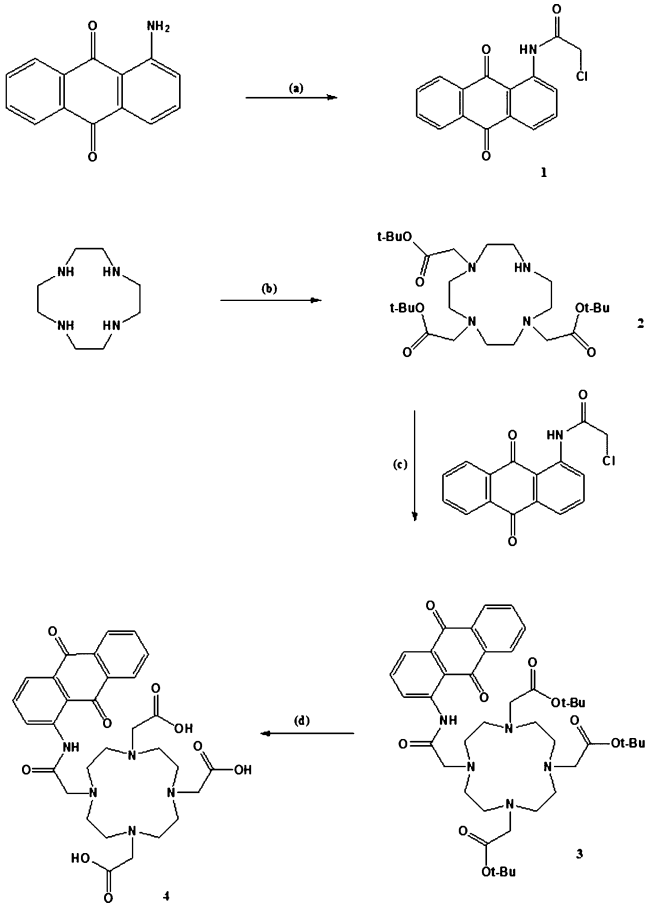

[a]Reagents and conditions: (a) 2-chloroacetyl chloride, pyridine, acetonitrile, 40 °C, 16 h; (b) *tert*-butylbromoacetate, acetonitrile, $NaHCO_3$, 0 °C, 48 h; (c) DIPEA, KI, toluene, 90 °C, 18 h; (d) DCM−TFA (1:1), 0 °C, 48 h.

*2-Chloro-N-(9,10-dioxo-9,10-dihydroanthracen-1-yl)-acetamide (**2**).* 1-Amino-9,10-anthraquinone (0.5 g, 2.24 mmol) and pyridine (300 μL) were taken in toluene (50 mL) and heated at 40 °C under nitrogen. A solution of 2-chloroacetylchloride (0.357 mL, 4.48 mmol) in toluene was added dropwise to it. The reaction mixture was allowed to reach 25 °C and left for overnight stirring. The solvent was evaporated under pressure, and the residue obtained was dissolved in 200 mL of $CHCl_3$. The organic layer was washed with water (3 × 50 mL) and dried over anhydrous Na_2SO_4. The solvent was removed under vacuum yielding compound **2** as a yellow powder. Yield: 0.460 g, 68.6%. ^{1}H NMR (400 MHz, $CDCl_3$): δ_H = 9.15 (dd, 1H, ArH), 8.30 (m, 1H, ArH), 8.20 (m, 1H, ArH), 8.10 (dd, 1H, *J* = 1.2 Hz, ArH), 7.75 (m, 3H, ArH), 4.31 (s, 2H, CH_2), 13.1 (1H, Br, NH) ppm, ^{13}C NMR (100 MHz, $CDCl_3$): δ_C = 187.09, 182.53, 166.39, 140.84, 135.75, 134.54, 134.41, 134.12, 133.87, 132.75, 127.59, 127.09, 126.03, 123.42, 118.58, 43.38 ppm. HR-ESI-MS calculated for $[C_{16}H_{10}ClNO_3 + H]^+$: 300.0427; found $[M + H]^+$: 300.0424. HPLC, System B, λ = 254 nm; t_R = 2.57 min.

*tert-Butyl-2,2′,2″-(10-(2-(9,10-dioxo-9,10-dihydroanthracen-1-ylamino)-2-oxoethyl)-1,4,7,10-tetraazacyclododecane-1,4,7-triyl)triacetate (**3**).* To a stirring solution of 1,4,7-tris(*tert*-butoxycarbonylmethyl)-1,4,7,10-tetraazacyclododecane (400 mg, 0.778 mmol) dissolved in toluene (100 mL) compound **2** (279 mg, 0.93 mmol) was added after the addition of KI (129 mg, 0.778 mmol) and DIPEA (0.2 mL) under an inert atmosphere. The reaction was heated at 90 °C for 18 h and monitored by TLC ($CHCl_3$:CH_3OH, 9:1) until completion of the reaction. The solvent was removed under vacuum, and chloroform was added to the oily residue which was further given wash with water (2 × 100 mL). The organic layer was collected separately and dried over Na_2SO_4, filtered, and evaporated, yielding an orange oil which was further purified using open column chromatography using eluent ($CHCl_3$/CH_3OH, 9:1) to give product **3**. Yield: 0.480 g, 80%. ^{1}H NMR (400 MHz, $CDCl_3$): δ_H = 12.38 (1H, NH), 8.95 (1H, s, ArH), 8.2 (2H, d, *J* = 5.2 Hz, ArH), 8.0 (1H, t, ArH), 7.8 (1H, t, ArH), 2.1−4.2 (24H, br, CH_2), 1.42 (27H, s, CH_3) ppm, ^{13}C NMR (100 MHz, $CDCl_3$): δ_C = 187.36, 182.47, 173.02, 172.95, 172.14, 141.42, 135.27, 134.72, 134.64, 134.11, 133.78, 132.71, 127.47, 127.14, 126.08, 122.83, 117.89, 81.85, 81.83, 57.98, 55.82, 55.71, 27.92, 27.87 ppm. HR-ESI-MS calculated for $[C_{42}H_{59}N_5O_9 + Na]^+$: 800.4210; found $[M + Na]^+$: 800.4181. HPLC, System B, λ = 254 nm; t_R = 4.21 min.

2,2′,2″-(10-(2-(9,10-Dioxo-9,10-dihydroanthracen-1-ylamino)-2-oxoethyl)-1,4,7,10-tetraazacyclododecane-1,4,7-triyl)triacetic acid, DO3A-Act-AQ. Compound **3** (100 mg) was added in a mixture of dichloromethane and trifluoroacetic acid (1:1), 10 mL at 0 °C. The reaction mixture was brought to 25 °C and further stirred for additional 48 h. The solvent was evaporated under vacuum, and the residue was dissolved in 2 mL of MeOH, followed by addition of 30 mL of diethyl ether at 0 °C and stirred for 1 h at room temperature producing a red precipitate of compound **4** which was further purified by preparative HPLC. Yield: 60 mg, 76%. ^{1}H NMR (400 MHz, MeOD): δ_H = 9.0 (1H, br, NH), 7.28−8.1 (7H, bm, ArH), 2.1−4.2 (24H, m, CH_2) ppm, ^{13}C NMR (100 MHz, DMSO-d_6): δ_C = 186.05, 182.02, 174.98, 170.00, 140.26, 136.85, 135.19, 123.08, 121.59, 118.51, 115.90, 113.15, 54.78, 51.16, 49.20 ppm. HR-ESI-MS calculated for $[C_{30}H_{35}N_5O_9 + Na]^+$: 632.2332; found $[M + Na]^+$: 632.2347. HPLC, System A, λ = 254 nm; t_R = 10.97 min.

Radiochemical Synthesis. Fresh $^{68}Ga^{3+}$ [$t_{1/2}$ 68 min] was eluted from ^{68}Ge/^{68}Ga generator system (IGG100, Eckert Ziegler, Germany) using 1 mL of 0.1 M HCl (740 MBq) and was trapped on a cation exchange Strata X-C cartridge column. The column was washed with 1 mL solution of 80% acetone/0.15 N HCl. ^{68}Ga desorbed from the column with 400 μL of 98% acetone/0.05 N HCl mixture. The pH of purified ^{68}Ga-(III) was adjusted to 4.0 using 1 M HEPES (2-[4-(2-hydroxyethyl)piperazin-1-yl]ethanesulfonic acid) buffer, and a stoichiometric amount 100 μg of DO3A-Act-AQ was added to the labeling vial. The mixture was heated at 90 °C for 10 min. It was cooled and passed through C-18 cartridge (preconditioned with C_2H_5OH and H_2O) to remove excess free ^{68}Ga by washing the cartridge with water (1 mL), and finally the compound was eluted from the cartridge with 200 μL of H_2O:C_2H_5OH (7:3). The labeling efficiency was checked by ITLC-SG in CH_3OH/NaOAc (1:1) and ACN/H_2O (1:1) solvent system.

Octanol−Water Partition Coefficient (log $P_{octanol/water}$). Log *P* was determined at physiological condition, pH 7.4 by the "shake-flask" method.[20] To a solution containing octanol (500 μL) and PBS (500 μL, pH 7.4) (obtained from saturated octanol-PBS solution), ^{68}Ga-DO3A-Act-AQ (50 μL, 1.85 MBq) was added. The resulting solution was vortexed at room

dx.doi.org/10.1021/mp4004089 | *Mol. Pharmaceutics* 2014, 11, 445−456

temperature and centrifuged at 4000 γ for 15 min. Aliquots of 10 μL were taken from both octanol and saline phases, and the activity was measured on a γ counter. The experiment was performed in triplicate. The partition coefficient (P) was calculated as log P.

In Vitro Studies. *Cell Culture.* Human brain malignant glioma (BMG-1) and human embryonic kidney (HEK) cells were procured from the National Centre for Cell Science, Pune and were maintained at 37 °C in a humidified CO_2 incubator (5% CO_2, 95% air) in RPMI 1640 and high glucose−DMEM, respectively. Cells were supplemented with 5% fetal bovine serum, 2 mM L-glutamine, 100 U/mL penicillin, and 100 μg/mL streptomycin. Cells (1×10^6) were regularly subcultured twice a week using 0.05% trypsin in 0.02% EDTA to maintain a log phase growth of cells.

Cell Viability Assessment. The cytotoxicity of DO3A-Act-AQ was assessed using the MTT colorimetric assay.[21] HEK and BMG-1 cells were seeded in 96-well plates (2×10^4 cells/200 μL per well) for 24 h. These cells were treated with DO3A-Act-AQ at different concentrations (0.0−0.5 mM) for different time periods (4 h, 24 and 48 h) at 37 °C. Untreated cells were used as a control. After treatment, cells were incubated with MTT (0.5 mg/mL) for 4 h at 37 °C at desired time intervals. The medium was then carefully removed by aspiration, and the cells were lysed in 200 μL of DMSO to dissolve the formazan crystals. The enzymatic reduction of MTT to formazan crystals was quantified by the optical density checked at 570 nm with 630 nm as a reference filter. The experiment was repeated three times, and results have been expressed as the mean ± SD.

Determination of Phosphatidylserine Externalization. Apoptosis induction in HEK and BMG-1 cells after treatment with DO3A-Act-AQ was studied by flow cytometry using Sigma (APOAF) annexin V-FITC apoptosis detection kit. Cells were seeded in 96-well plates (1×10^3) cells per well and incubated at 37 °C for 24 h. The stock solution (10 mM) of DO3A-Act-AQ was diluted with culture medium to a total volume of 300 μL. Untreated cells were used as a control. Cells were treated with 0.1 mM DO3A-Act-AQ. Cells were collected by centrifugation (10 min, 1000 γ) after harvesting, washed with PBS again, and resuspended in annexin-binding buffer (10 μg/mL HEPES, 140 μg/mL NaCl, and 2.5 μg/mL $CaCl_2$, pH 7.4). Afterward, 5 μL of the annexin V conjugate was added to each sample and 5 μL of PI staining solution (1 μg/mL). Cells were incubated at room temperature for 15 min in dark. Flow cytometric analysis was made within one hour of addition of annexin-binding buffer to each tube. Annexin V-FITC fluorescence was collected on the FL-1 channel, and PI fluorescence was collected on the FL-2 channel on the log scale. A minimum of 10 000 cells per sample were acquired and analyzed using Cell Quest software.

Cell Cycle Analysis. Exponentially growing cells (HEK and BMG-1) were treated with 0.1 mM of DO3A-Act-AQ for 4 and 24 h. Cells were collected by trypsinization and washed twice in ice-cold PBS at pH 7.4. Cell suspensions were fixed by vigorous addition of ice-cold 70% (v/v) ethanol and stored at 4 °C for a minimum of 24 h prior to analysis. Cells at a density of approximately 1×10^6 were treated with 200 μg/mL RNase A for 30 min at 37 °C followed by 200 μL of propidium iodide staining solution (20 μg/mL propidium iodide in PBS at pH 7.4) and incubated in the dark at room temperature for 10−15 min. The percentage of cells in sub-G_1, G_0/G_1, S, and G_2/M phases of cell cycle was determined and analyzed from at least three independent experiments using Cell Quest (version 3.0.1: Becton, Dickinson, and Co., Franklin Lakes, NJ) and ModFit LT (version 2.0: Verity Software, Inc., Topsham, ME, USA) software for acquisition and analysis. The analysis was done in triplicate.

In Vitro Stability. The *in vitro* stability of ^{68}Ga-DO3A-Act-AQ was checked at the physiological pH. The complex was incubated with PBS, and the ITLC was checked at different time intervals up to 4 h to determine the stability of conjugate in PBS. Further, serum stability was estimated using blood samples collected from healthy volunteers by venipuncture which was allowed to clot for almost 45 min at 37 °C in a humidified incubator at 95% air/5% CO_2. The blood samples were centrifuged, and the human serum was collected by filtration through 0.22 μm syringe filter. Human serum (1 mL) was incubated with 50 μL of ^{68}Ga-DO3A-Act-AQ (3.7 MBq), and dissociation of the complexes was determined after 30, 60, 120, 180, and 240 min by running an ITLC using methanol−ammonium acetate (1:1) as the developing solvent.

CD Spectroscopic Measurements. All CD spectroscopic measurements were carried out with a continuous flow of nitrogen purging the polarimeter, and the measurements were performed at room temperature with 1 cm pathway quartz cells. The CD spectra were run from 320 to 220 nm at a speed of 20 nm/min, and the buffer (5 μg/mL Tris−HCl, pH 7.4) background was automatically subtracted. Data were recorded at an interval of 0.1 nm. The CD spectrum of CT-DNA alone (0.05 mM) was recorded as the control. The results were taken as ellipticity in mdeg, and scans were accumulated and automatically averaged. The concentration of CT-DNA was kept constant at 0.05 mM, while 0.1 mM of compound in buffer solution was added to CT-DNA (1:1).

Photophysical Properties. UV−vis absorbance and fluorescence emission spectrum for DO3A-Act-AQ was measured to check the $\lambda_{absorbance}$ and $\lambda_{excitation}$ and $\lambda_{emission}$ range. A stock solution of concentration 1 mM was prepared in PBS buffer, and dilutions were done as per the requirement. A spectrum was recorded from 200 to 800 nm range. The dilution prepared was in the range of 10−70 μM.

Fluorescence Spectroscopic Studies. The fluorescence emission spectra were measured at 298 K in the wavelength range of 300−800 nm. Blanks corresponding to the Tris-HCl buffer solution (pH 7.4) were subtracted to correct background fluorescence. Increasing concentrations of compound (0.1−0.4 mM) was micropipetted directly into a 1.0 cm cell containing 0.005 mM ethidium bromide and 0.5 mM CT-DNA (total volume 1 mL), and the reaction was performed at room temperature. The synchronous fluorescence spectra was recorded by scanning both excitation and emission wavelengths simultaneously. The spectrofluorometric measurements of all samples were carried out over the excitation wavelength range of 200−700 at 1 nm intervals, and $\Delta\lambda$ (a constant wavelength interval between emission and excitation wavelength) was changed in the range of 10−200 at 10 nm intervals (total of 20 $\Delta\lambda$ increments). The EB-DNA system was excited at 530 nm, and the emission spectrum was taken at 604 nm. The relative binding of the compound with CT-DNA was determined by using classical Stern−Volmer equation

$$I_o/I = 1 + K_{sv}[\text{compound}]$$

where I_o and I are the fluorescence intensity in absence and presence of the quencher, K_{sv} is the Stern−Volmer quenching constant, and [compound] is the concentration of the compound.

The apparent binding constant (K_{app}) was also calculated from the equation,

$$K_{EB}[EB] = K_{app}[compound]$$

where the complex concentration was the value at a 50% reduction of the fluorescence intensity of EB and K_{EB} = 1.0 × 10^7 M^{-1} [EB] = 5.0 μM.

The stock solution of CT-DNA was prepared freshly in 5 μg/mL Tris-HCl buffer, pH 7.4. The purity of the DNA was checked by observing the ratio of the absorbance at 260/280 nm. The solution gave a ratio of >1.8 at A_{260}/A_{280}, which indicates that DNA was sufficiently free from protein. The concentration of DNA in stock solution was determined by UV absorption at 260 nm using a molar absorption coefficient ε_{260} = 6600 L mol^{-1} cm^{-1}.

Potentiometric Titration. A pH meter−electrode system was calibrated for pH 4, 7, and 9 using Metroholm ion analysis buffers before the titrations. The protonation constant of DO3A-Act-AQ were determined potentiometrically by titrating 1 mM of DO3A-Act-AQ with 0.1 mM tetramethylammonium hydroxide (TMAOH). Titrations were performed in the pH range of 2−11.5 for protonation constants. The complexation constants of DO3A-Act-AQ with Sm(III), Lu(II), Cu(II), and Ga(III) were determined by direct pH potentiometric titration (2−4 mM M^{n+} and 2 mM ligand solutions), I = 0.1 g/L using TMACl. Metal solutions were prepared by dissolving the quantitable amounts of their salts in Milli-Q water. For titrations of complexes, a 1:1 ligand to metal ratio was prepared, and the experiment was performed in duplicate. The protonation and stability constants were evaluated from titration data using the program *Tiamo* 2.0.

Animal Model. All animal experiments were performed in accordance with guidelines of Institute's Animal Ethics Committee (Reg. No. 8/GO/a/99/CPCSEA). For blood clearance study, male New Zealand rabbits were used, and athymic nude mice were used for PET imaging and *ex vivo* biodistribution studies. Animals were housed under conditions of controlled temperature of 22 ± 2 °C and normal diet. Mice were inoculated subcutaneously with 0.1 mL of cell suspension of BMG-1 (1 × 10^6 cells) in the right front flank under sterilized condition. When the tumor volume reached ∼400 mm^3 (after 3−4 weeks of inoculation), the BMG-1 tumor-bearing mice were used for biodistribution and imaging studies.

Blood Kinetics Study. The blood kinetics was carried out in male albino New Zealand rabbit weighing approximately 2.6−3.0 kg to study the clearance of the radiolabeled complex from the blood circulation. 37.0 MBq of radiolabeled compound was injected intravenously through the dorsal ear vein of the rabbit and blood samples (0.3 mL) were taken from the other ear vein at different time interval starting from 10 min until 240 min, and counts were monitored on a gamma counter. Whole body blood was considered to an amount equal to 7.3% of the body weight of the rabbit. Data were expressed as percent administered dose at different time intervals.

Ex vivo Biodistribution Study. The biodistribution of ^{68}Ga-DO3A-Act-AQ was studied in six weeks old female athymic nude mice weighing approximately 20 g. An intravenous injection of ^{68}Ga-DO3A-Act-AQ in a volume of 100 μL (9.25 MBq) was injected through the tail vein, and mice were sacrificed at 1, 2, 3, and 4 h time intervals post injection. Blood was collected by cardiac puncture, and all other different organs, heart, lung, liver, spleen, kidneys, stomach, and muscle were removed and washed with normal saline to remove surface blood and debris from the organs. Organs were weighed, and the radioactivity was measured. The uptake of ^{68}Ga-DO3A-Act-AQ in each tissue was calculated and expressed as percentage injected dose per gram of the tissue.

Scintigraphic Studies. PET imaging was performed on athymic nude mice bearing tumor from BMG-1 cells xenografts grown for 14 days on right forelimb (100−200 mm^3). ^{68}Ga-DO3A-Act-AQ (3.7 MBq, 100 μL) was injected through a tail vein of the animal to visualize the tumor uptake. PET images were taken at 120 min post injection.

Statistical Analysis. Results are depicted as the mean ± standard error of the mean (SEM). Statistical analysis was performed using a Student's t test. $P < 0.05$ was considered significant.

RESULTS

Synthesis, Radiolabeling, Partition Coefficient, and *in Vitro* Stability. The potential of anthraquinone to control cellular proliferation through DNA binding was utilized for tumor targeting by conjugating it with macrocyclic, 1,4,7,10-tetraazacyclododecane based chelating system. The synthesis of DO3A-Act-AQ involves the conjugation of DO3A unit by means of a linker to an anthraquinone moiety. 2-Chloroacetyl chloride was chosen as source of linkage and was reacted with 1-aminoanthraquinone to give the α-chloramide, 2-chloro-*N*-(9,10-dioxo-9,10-dihydroanthracen-1-yl)-acetamide, **2**, in 68.6% yield. 1,4,7-Tris(carboxymethyl)-1,4,7,10-tetraazacyclododecane, **1** (80%), was synthesized by reaction of *tert*-butylbromoacetate on 1,4,7,10-tetraazacyclododecane. The fourth unsubstituted arm of DO3A was conjugated with 2-chloro-*N*-(9,10-dioxo-9,10-dihydro-anthracen-1-yl)-acetamide in the presence of DIPEA to yield compound **3** in 80% yield. The progress of the reaction steps was checked through TLC in solvent system 9.5:0.5 (DCM−CH_3OH). The compound **3** was characterized by NMR spectroscopy wherein the ^{1}H spectrum data clearly shows the entire seven protons of anthraquinone in aromatic region of 7.8−8.9 ppm. While the 24 methylene protons in the region of 2.1−4.1 ppm along with the 27 protons of methyl group at 1.5 ppm confirms the conjugation.

Later, *tertiary* butyl groups of compound **3** were cleaved using (1:1) TFA−DCM to obtain the desired compound, 2,2′,2″-(10-(2-(9,10-dioxo-9,10-dihydroanthracen-1-ylamino)-2-oxoethyl)-1,4,7,10-tetraazacyclododecane-1,4,7-triyl)triacetic acid in 76% yield after purification. The precursors and final compounds were characterized by ^{1}H, ^{13}C, and high resolution mass spectrometry (Figures S1−S12 in the Supporting Information). ^{68}Ga labeling was performed in a straightforward method with a preparation time for ^{68}Ga-DO3A-Act-AQ of 20 min at 90 °C with a good radiochemical yield (84%) and a specific activity of 4.62 MBq/nmol. The maximum radiochemical yield was observed at pH 4.0 using HEPES buffer, after heating for 10 min at 90 °C. The radiochemical purity was greater than 95%, with DO3A-Act-AQ binding to Ga^{3+} quantitatively to provide a single radiolabeled product as monitored by radio-TLC using 50% aqueous acetonitrile solvent as shown in Figure 1. After radiolabeling traces of free Ga^{3+} from the reaction mixture were removed by passing the labeled compound on a C-18 cartridge followed by washing with water. ^{68}Ga-DO3A-Act-AQ was eluted from the C-18 cartridge with H_2O−C_2H_5OH (7:3) which further enhanced on increasing the elution volume from 100 to 200 μL. The partition coefficient, log P (pH 7.4), of complex was determined by the "shake-flask" method using 1-octanol-to-

dx.doi.org/10.1021/mp4004089 | *Mol. Pharmaceutics* 2014, 11, 445−456

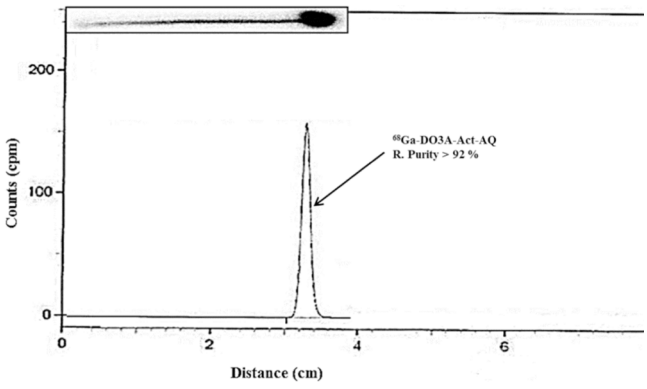

Figure 1. Radio-TLC of ^{68}Ga-DO3A-Act-AQ in the ACN−water (1:1) solvent system.

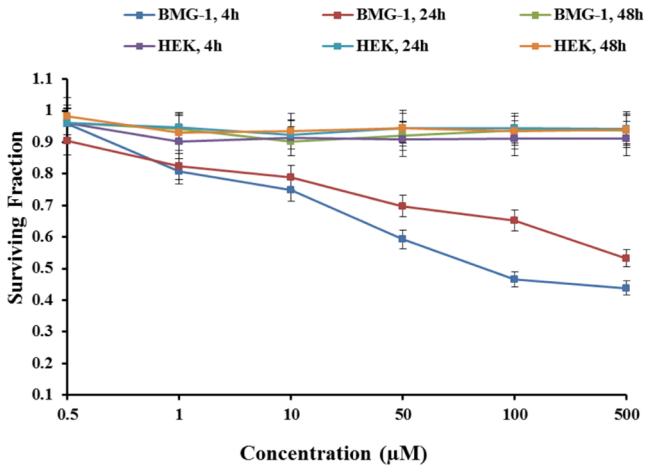

Figure 2. Colorimetric estimation for the cytotoxicity of DO3A-Act-AQ with respect to time (4, 24, and 48 h) and concentration (0.5, 1, 10, 50, 100, 500 μM) in HEK and BMG-1 cell lines.

PBS and was found to be −1.67 ± 0.2. To check the stability of the complex at physiological conditions, the complex was incubated with PBS buffer (pH 7.4). The probe was stable up to 2 h at physiological condition as no free ^{68}Ga was detected by the radio TLC. For *in vitro* serum stability analysis, the probe was challenged with the proteins present in serum (albumin and transferrin). More than 92% of the radioactivity was found to be associated with the conjugate even after 2 h incubation at 37 °C. After 2 h ^{68}Ga-DO3A-Act-AQ exhibited 13.7% transcomplexation in human serum which increased to 14.3% after 4 h of challenge suggesting serum stability up to 2 h (Figure S13 in the Supporting Information).

Cell Viability Assay. The cytotoxic effect of DO3A-Act-AQ was determined on two cell lines, BMG-1 and HEK cells, by an MTT assay. Time and concentration dependence on cytotoxicity was analyzed by cell viability data (surviving fraction) at different concentrations (0.05−0.5 mM) and time intervals (4, 24, and 48 h). At lower concentrations no sign of cytotoxicity was seen in either cell lines. HEK cells showed nonsignificant cell death after 24 h of treatment (0.05 mM), and the surviving fraction decreased from 0.971 ± 0.01% to 0.930 ± 0.03%, whereas BMG-1 cells on incubation with DO3A-Act-AQ (0.05 mM) exhibited a significant reduction in survival (59.0 ± 0.5%) after 4 h which further decreased to 43.0 ± 0.11% on increasing the concentration to 0.5 mM. DO3A-Act-AQ displayed a time- and dose-dependent toxicity toward BMG-1 cells as shown in Figure 2.

Phosphatidylserine Externalization. The ability of DO3A-Act-AQ to induce apoptosis in BMG-1 and HEK cells was ascertained through flow cytometry. Phosphatidylserine externalization/apoptosis was examined after 4 and 24 h of treatment with DO3A-Act-AQ (0.1 mM) as shown in flowcytometric plot in Figure 3. Here, Q1 quadrant represents cells having high affinity for annexin V, simultaneous binding of annexin V, and propidium iodide represents Q2 quadrant, indicating cells in late apoptosis; Q3 represents live cells, and Q4 are solely stained with PI and corresponds to necrotic cells. Treatment of DO3A-Act-AQ on BMG-1 cells resulted in an increase in early apoptotic cells ($FITC^+/PI^-$) to 23.8% (4 h) in comparison to 0.1% in control which reached to 26.3% after 24 h of treatment, whereas late apoptotic cell population ($FITC^+/PI^+$) displayed a significant increase from 0.2% at 0 h to 16.9% at 24 h as shown in Figure 4. However, in HEK cells, cells undergoing early apoptosis in $FITC^+/PI^+$ fraction showed a marginal increase from 0.4% in control cells to 1.3% after 4 h and 2.0% after 24 h of treatment. Also, a 3-fold increase fold in late apoptotic cell population after 4 h was noticed in HEK cells which decreased nonsignificantly at late time point of 24 h. After 4 h, a necrotic BMG-1 cell population showed a 47-fold increase which was 2.3-fold in HEK cells.

Cell Cycle Analysis. Cell cycle analysis was performed on HEK and BMG-1 cells after 4 and 24 h on treatment with DO3A-Act-AQ (0.1 mM). A measurable change at various phases of cell cycle was observed post 4 h treatment. BMG-1 cells in the G_1 phase decreased to 53.27% from 58.47%, while an increase in HEK cell population in the G_1 phase from 34.2% to 59.31% was observed. A significant increase in cellular population was observed in the S phase of BMG-1 cells (6.09% in control to 17.77% in 4 h), but HEK cell population decreased from 16.59% to 6.66%.

The distribution of cells in different phases post 24 h treatment suggested increase in BMG-1 cells in S phase to 26.94% with concomitant increase of 8.88% of HEK cells (Figures 5 and 6). In G_1 phase population of BMG-1 cells came down to 35.32%, while an unsubstantial change was seen in HEK cells. BMG-1 cells also exhibited 8-fold increases in sub G_1 phase cell population (0.84% in control to 6.41% after 24 h); however, the apoptotic HEK cell population decreased with time and reaches to 0.24% (after 24 h) compared to 1.09% in control.

Photophysical Results. UV−vis and fluorescence spectroscopy studies were performed on DO3A-Act-AQ at different concentration ranges (0.01−0.07 mM). The concentration range of DO3A-Act-AQ was optimized for performing fluorescence and absorption studies, and the suitable window for the studies was found in the region 0.01 mM. Absorbance and fluorescence bands were observed which enhanced on progressive increase in concentration (hyperchromic shift. The $\lambda_{absorption\text{-}max}$ was found at 393 nm, while $\lambda_{excitation\text{-}max}$ and $\lambda_{emission\text{-}max}$ were observed at 415 nm and 543 nm, respectively (Figure S14 in the Supporting Information).

DNA Binding Study Using Fluorescence and CD Spectroscopy. The binding of DO3A-Act-AQ with CT-DNA was studied by evaluating the fluorescence emission intensity of the ethidium bromide−DNA system upon successive addition of the DO3A-Act-AQ which acted as quencher. The fluorescence quenching profile of EB bound to DNA on addition of DO3A-Act-AQ is shown in Figure 7 in which the fluorescence intensity at 610 nm ($\lambda_{excitation\text{-}max}$ 518 nm) of EB in the bound form was

dx.doi.org/10.1021/mp4004089 | *Mol. Pharmaceutics* 2014, 11, 445−456

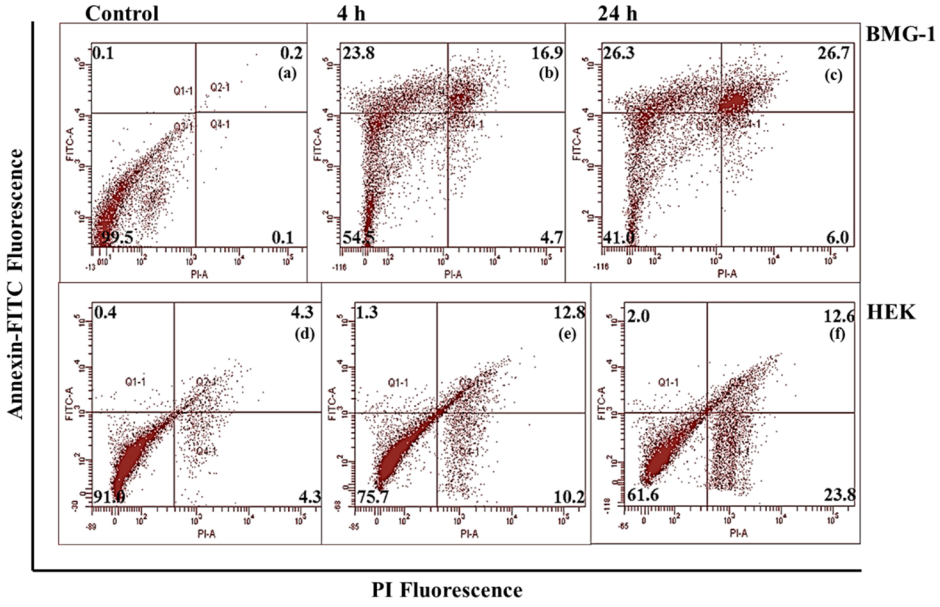

Figure 3. Flow cytometric plots of BMG-1 (a, b, c) and HEK (d, e, f) cells in the presence of annexin-V/propidium iodide (PI) after treatment with DO3A-Act-AQ (0.1 mM) at 4 and 24 h.

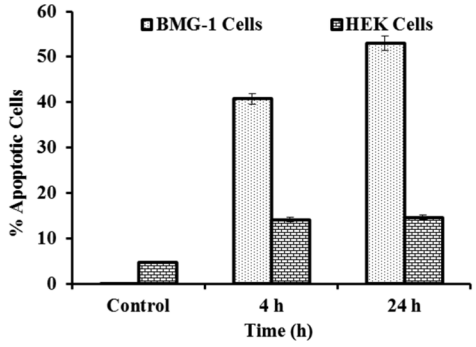

Figure 4. Apoptosis in HEK and BMG-1 cells at different time intervals (4 and 24 h) after treatment with DO3A-Act-AQ (0.1 mM).

plotted against the compound concentration and found to be in agreement with a Stern−Volmer plot of I_o/I vs [DO3A-Act-AQ] (Figure S15 in the Supporting Information). The quenching constant was found to be 2.4157×10^6 L mol^{-1}. The apparent binding constant K_{app} was determined to be 1.25×10^6 M^{-1}. The CD spectrum of CT-DNA after addition of DO3A-Act-AQ in a ratio of (1:1) demonstrated a decrease in the intensity of both the positive band at 275 nm and the negative band at 248 nm as shown in Figure S16 in the Supporting Information.

Protonation and Thermodynamic Stability Constant. The protonation and stability constant of complex of DO3A-Act-AQ with Cu(II), Ga(III), and therapeutic metals like Sm(III) and Lu(III) was determined by potentiometric titration over the pH range 2−11.5. A pH-potentiometric titration of the ligand DO3A-Act-AQ gave three protonation constants at 9.66, 8.07, and 5.87 which were likely to be due to the three carboxylic acid groups present in the structure. The stability constant of DO3A-Act-AQ for Sm^{3+}, Lu^{3+}, Ga^{3+}, and Cu^{2+} were found to be 19.5, 18.5, 19.3, and 11.6, respectively, and shown in Tables 1 and 2. The values obtained for protonation constant were found to be in accordance of the previously reported value of DOTA. The stability constant with Ga(II) and therapeutic metals Sm(III) and Lu(III) were in accordance of previously reported value of DOTA; however, with Cu(II) it was found to be less.[22]

Blood Kinetics Study, Ex Vivo Biodistribution, and PET Imaging. The blood clearance studies of ^{68}Ga-DO3A-Act-AQ performed in normal rabbits displayed a biphasic clearance pattern from blood circulation and 70.3% of injected activity washed out from the circulation at 30 min post injection as shown in Figure 8. The percentage of residual activity in blood circulation at 2 h was 13.61 ± 0.01% which further decreased to 9.42 ± 0.04% at 4 h p.i. Thus, blood clearance of complex from circulation followed a biphasic mode with activity rapidly clearing in the initial phase followed by a slow phase later. Biological half-lives $t_{1/2}$(fast) and $t_{1/2}$(slow) were found to be 40 ± 0.3 min and 3 h 40 min ± 0.1 min, respectively. The PET/CT studies were carried out using an integrated PET/CT scanner on athymic nude mice xenografted with BMG-1 cells at different time intervals. The mice injected with ^{68}Ga-DO3A-Act-AQ exhibited accumulation at the site of tumor within 1 h which reached maximum in 2 h (Figure 9). Prominent abdominal uptake was observed; however, a quick washout from liver was also seen. ^{68}Ga-DO3A-Act-AQ was checked *ex vivo* for their pharmacokinetics on athymic nude mice xenografted with BMG-1 cells. The biodistribution studies were performed at various time intervals between 30 and 240 min. The study was useful for the screening of biological profile and to assess the potential of complex in achieving the objective. Data from these studies are shown in the graphical form in Figure 10. The accumulation of ^{68}Ga-DO3A-Act-AQ in kidney and liver was 6.21 ± 0.03 and 3.6 ± 0.01 at 30 min p.i. The localization in stomach and intestine was lower than 1.2% after 1 h p.i. The study reveals good accumulation of the complex in tumor which reached maximum after 2 h with value of 1.85 ± 0.03%. After 3 h, localization of activity was second highest in tumor (1.2 ± 0.32) after kidney (2.31 ± 0.21). The accumulation in tumor decreased to 0.98 ± 0.34 after 4 h. The ratio of tumor to soft tissue (muscle) was found to be 1.72 at 30 min which increased to 8.40 after 2 h of administration.

dx.doi.org/10.1021/mp4004089 | *Mol. Pharmaceutics* 2014, 11, 445−456

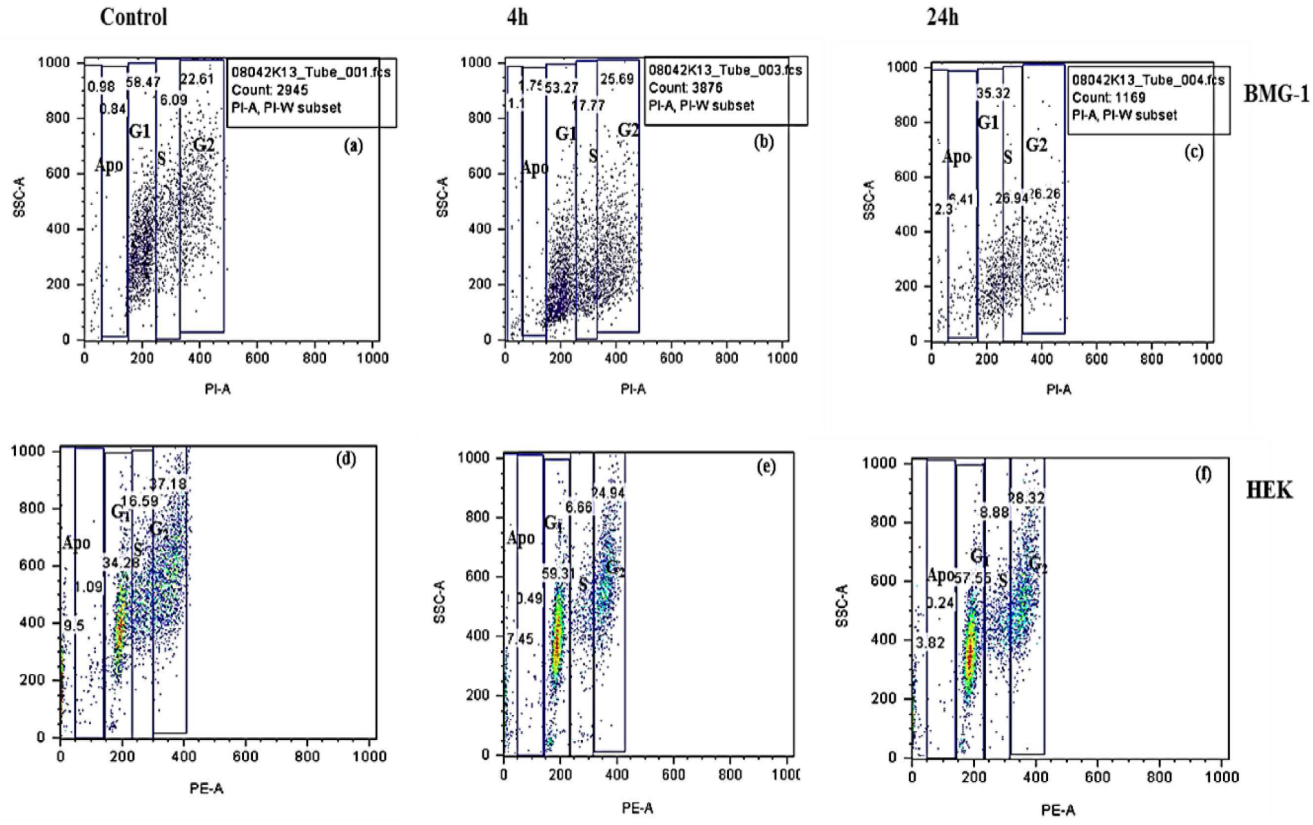

Figure 5. (a–f) Cell cycle analysis of BMG-1 and HEK cells treated with DO3A-Act-AQ (0.1 mM) at different time intervals (4 and 24 h).

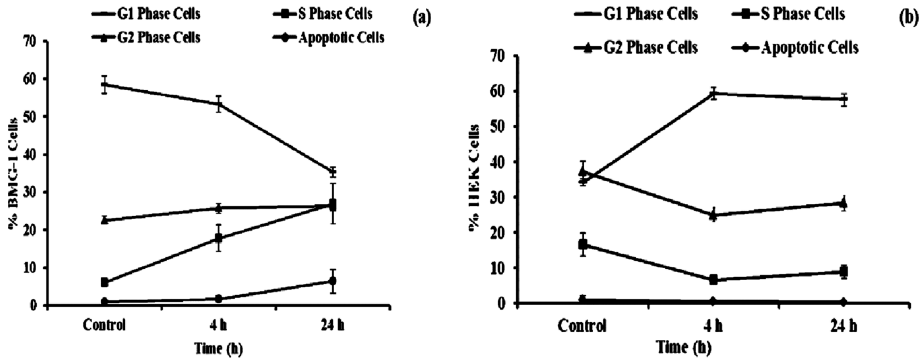

Figure 6. Cell cycle distribution of HEK and BMG-1 cells on different stages following treatment of DO3A-Act-AQ (0.1 mM) after 4 and 24 h. The percentage of cells in different phases of the cell cycle was analyzed using Mod fit software.

DISCUSSION

Anthraquinone-based compounds that inserts between the two base pairs present in the DNA double helix and culminates to cell death have demonstrated amazing potential in cancer chemotherapy.[23,24] Similarly, 1,4,7,10-tetraazacyclododecane-1,4,7,10-tetraacetic acid (DOTA) forms high *in vitro* and *in vivo* stable radiometal (M^{3+}) labeled complexes.[25,26] Thus it was thought worthwhile to utilize the DNA intercalating properties of anthraquinone in the detection and treatment of tumors. A facile synthetic strategy was used where 1,4,7-tris-(carboxymethyl)-1,4,7,10-tetraazacyclododecane (DO3A) is conjugated with anthraquinone derivative, 2-chloro-*N*-(9,10-dioxo-9,10-dihydro-anthracen-1-yl)-acetamide to finally obtain 2,2′,2″-(10-(2-(9,10-dioxo-9,10-dihydroanthracen-1-ylamino)-2-oxoethyl)-1,4,7,10-tetraazacyclododecane-1,4,7-triyl)triacetic acid (DO3A-Act-AQ) as the product, and its cytostatic/cytotoxic behavior and specificity toward tumor was studied and compared with known derivatives. The synthesis of probe DO3A-Act-AQ was confirmed through ^{1}H NMR by presence of peaks in the region of 7.8–8.1 and 3.2–4.2 ppm corresponding to 7 H of aromatic anthraquinone moiety and 24 H of the DO3A unit, and the $[M + Na]^{+}$ peak at 632.2347 further supported the successful formation of DO3A-Act-AQ.[27] The three protonation constant values (9.66, 8.07, and 5.87) corresponding to three carboxylic acid groups present in probe were in range of other known derivatives of DOTA further supported the synthesis of DO3A-Act-AQ an suggested no effect of anthraquinone on the chemical properties of DO3A. ^{68}Ga is a ^{68}Ge/^{68}Ga generator system β^{+} emitting radionuclide with a half-life of 68 min and is a promising candidate for application in positron emission tomography (PET) requiring no on-site cyclotron facility, making it economic. Unlike other

dx.doi.org/10.1021/mp4004089 | *Mol. Pharmaceutics* 2014, 11, 445–456

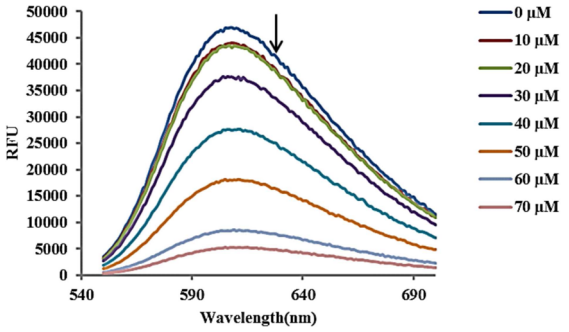

Figure 7. Emission spectra of EB (5.0 μM) bound to CT−DNA (50 μM) in the absence and presence of compound, (r = 0, 0.2, 0.4, 0.6, 0.8, 1.0, 1.2, and 1.4), r = [compounds]/[CT−DNA]. Arrows show the intensity changes upon the addition of increasing concentrations of DO3A-Act-AQ, respectively. $\lambda_{excitation\text{-}max}$ = 518 nm.

Table 1. Protonation Constant (log K) of DOTA, DTPA, and DO3A-Act-AQ in NMe_4Cl (0.1 M) at 298 K

	DOTA	DTPA	DO3A-Act-AQ
log K_1H	11.14	10.49	9.66
log K_2H	9.69	8.37	8.07
log K_3H	4.85	4.09	5.87

Table 2. Stability Constant (log β) of Metal Complexes of DOTA and DO3A-Act-AQ (298 K, μ = 0.1 M, NMe_4Cl)

	DOTA	DO3A-Act-AQ
log β_{GaL}	21.3	19.3
log β_{CuL}	22.2	11.6
log β_{SmL}	23.0	19.5
log β_{LuL}	25.4	18.5

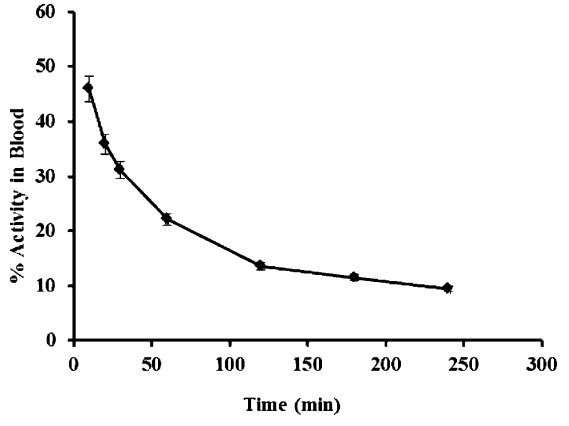

Figure 8. Blood clearance of ^{68}Ga-DO3A-Act-AQ (37.0 MBq) activity administered through ear vein in normal New Zealand rabbit.

PET radioisotopes like ^{11}C or ^{18}F, ionic Ga^{3+} cannot be bound covalently to targeting biological vectors but must be complexed by a ligand which is conjugated to the vector giving an advantage that labeling can be performed just prior to *in vivo* evaluation, and loss of activity is thus kept to a minimum. Thus DO3A-Act-AQ with DO3A backbone was utilized for PET imaging post labeling with ^{68}Ga. ^{68}Ga-DO3A-Act-AQ was prepared in high radiochemical purity (>94%) and radiochemical yield (84%) with a specific activity of 4.62 MBq/nmol. The optimum complexation yield for $^{68}Ga^{3+}$ with DO3A-Act-AQ was achieved in the pH range of 3.5−4.0 using nonionic

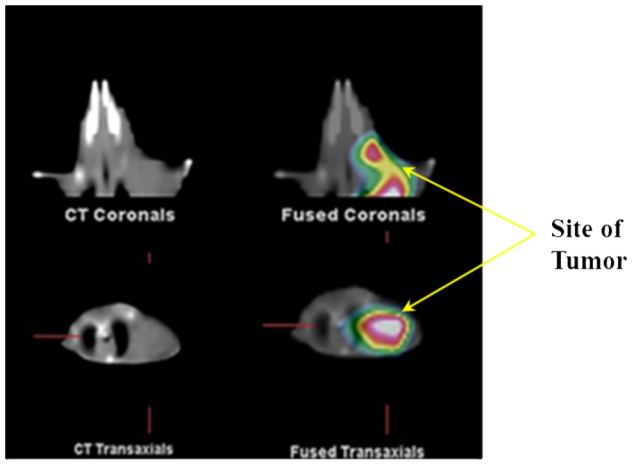

Figure 9. PET/CT images of athymic nude mice (xenografted with BMG-1 cells on front right flank) after 2 h showing coronal and transaxial images.

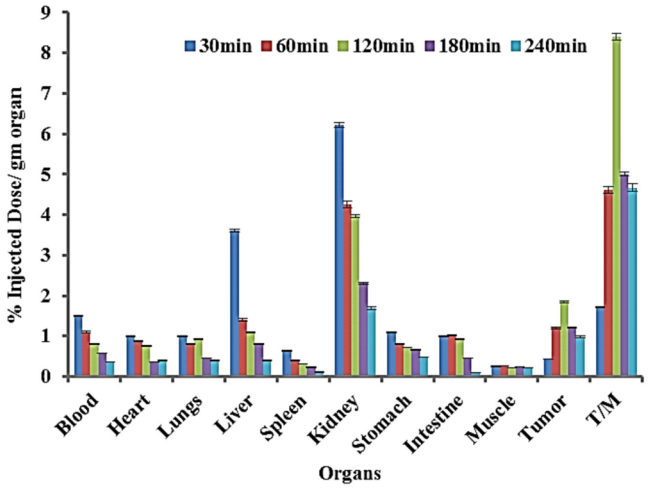

Figure 10. Biodistribution of ^{68}Ga-DO3A-Act-AQ performed on female athymic nude mice bearing BMG-1 tumor on the right front flank at different time intervals (30, 60, 120, 180, and 240 min).

buffer HEPES. A higher pH resulted in inferior radiolabeling, probably due to the formation of hydroxide species. Similarly, a temperature lower than 90 °C reduced the radiochemical yield to almost 40% at 55 °C as higher reaction temperatures enhance the complexation of less reactive Ga^{3+} species, that is, partly oxygenated species.[28] Radio-TLC analysis suggested formation of ^{68}Ga-DO3A-Act-AQ as the major species (>95%) which was suitable enough to proceed for further studies. DOTA derivatives are known for stable gallium complex formation, which was further confirmed by high stability constant value (21.3) with Ga^{3+}.[29] *In vitro* stability of ^{68}Ga-DO3A-Act-AQ was established in PBS (pH 7.4) with >94% intact radiotracer as no significant detachment from the radiolabeled complex was observed on ITLC even after 4 h incubation at physiological condition. Since the title compound was designed for tumor thus consequently, investigation on its tumor binding affinity was of prime importance along with its pharmacokinetics. Strong serum protein binding, that is, $^{68}Ga^{3+}$-transferrin complex in comparison to ^{68}Ga-labeled complex, often leads to a delay in blood clearance, resulting in a low target-to-background ratio; besides human plasma enzyme also tends to decompose the exogenous compounds, so

dx.doi.org/10.1021/mp4004089 | *Mol. Pharmaceutics* 2014, 11, 445−456

a binding study with human serum protein is a requirement for the correct prediction of the biological importance of the probe.[30] *In vitro* serum stability of DO3A-Act-AQ was assessed and found to be more than 90% after 2 h of incubation with human serum at physiological pH, making it appropriate to avoid background activity due to dissociation of the metal ion. MTT assay on HEK cell line predicts limited toxicity on normal cells inducing 10% toxicity after 24 h of treatment (0.1 mM) ensuring its suitability for imaging purpose. *In vivo* blood clearance exhibited a biphasic clearance pattern in blood kinetics data of ^{68}Ga-DO3A-Act-AQ which could be contributed to low lipophilicity of probe. Biological distribution studies were performed in athymic nude mice, and the percentage of injected dose associated with each organs was calculated based on the activity measured/g organ or tissue. The biodistribution study suggested prominent uptake of ^{68}Ga-DO3A-Act-AQ in kidneys at all measured time points suggesting renal excretion route of the probe. As anthraquinone derivatives are mainly metabolized through liver, the activity was found high (3.6 ± 0.01%) in liver at 30 min which got significantly reduced to 1.4 ± 0.2% within 1 h. The uptake in liver decreased faster than kidney with time and no prominent accumulation was observed in other organs like the lungs, spleen, heart, stomach, and intestine. The accumulation of ^{68}Ga-DO3A-Act-AQ at the site of tumor is seen at an early time point (1.2 ± 0.01%, 1 h) which reached to a maximum (1.85 ± 0.03%) at 2 h and remained significant up to 3 h. The tumor-to-muscle ratio was 8.4-fold which further demonstrated the potential of this hybrid compound as a tumor-seeking agent. The imaging studies further provide strong support to the tumor targeting ability of the developed probe.

The well-known DNA intercalating property (cytostatic/cytotoxic nature) of anthraquinone, which is being exploited in cancer chemotherapy to control cellular proliferation, was investigated on DO3A-Act-AQ.[31−34] The *in vitro* toxicity of DO3A-Act-AQ toward neuroblastoma cells was compared with healthy nephritic cells. The probe (0.1 mM) induced cellular death in BMG-1 cells with only 47% cell viability was observed after 24 h; however, no significant sign of cellular death was seen in HEK cells, corroborating its specificity toward cancer cells. The IC_{50} of simple 1,4-diamido anthraquinone derivative on C6 (glioma) cells (>10 μM) were related with probe's toxicity toward BMG-1 cells (0.1 mM).[35] The high IC_{50} value of the conjugate was probably due to the conjugation of DO3A moiety to the anthraquinone.[35−39] As reported in literature, anthraquinone derivatives induce apoptosis in cancer cells at the micromolar range.[40] Thus flow cytometry studies performed on BMG-1 cells at IC_{50} showed an increase of 263-fold in early apoptosis cells, whereas HEK cells displayed a nonsignificant increase of 5-fold after 24 h of treatment with probe as compared to gastric cancer cell line after 24 h, which showed 4.2-fold increase on treatment with 25 ng/mL of triazole derived anthraquinone derivatives.[31] BMG-1 cells displayed an approximate 8-fold increase in sub-G1 level which is an indicator of apoptotic cell population. However, a decrease of 4.5% was observed in the sub-G_1 phase of HEK cells after 24 h. A significant increase in the cell population from 6.09% to 26.94% after 24 h in the S phase revealed that BMG-1 cells could arrest cell population in the S phase with time. However a transient G_1 phase arrest was seen initially in HEK cells, which released at a later time point. Cell cycle results were found to be supporting annexin V apoptosis results, as the necrotic cell population in HEK cells could be due to the marginal G_1 and S and G_2 phase arrest after 4 and 24 h. These results were found to be better than 1,3-substituted anthraquinone derivatives which were inducing G_2/M phase arrest in NTUB1 cells (a human bladder carcinoma cell line),[41] thus ensuring retained anticancer property of the compound as evident by apoptosis induction along with S phase arrest in cancer cells after 24 h of treatment. The therapeutic behavior of anthraquinone derivatives are known by DNA binding nature. The efficacy of the developed molecule was checked by performing DNA binding studies with fluorescence and CD spectroscopic techniques under physiological conditions. It is already well-known that the emission intensity of ethidium bromide dye enhances upon DNA intercalation.[42] A reduction in emission intensity was observed upon progressive addition of DO3A-Act-AQ (10−70 μM) due to the substitution of bound ethidium bromide from the EB-DNA system with DO3A-Act-AQ. The Stern−Volmer quenching constant, K_{sv}, and apparent binding constant, K_{app}, of DO3A-Act-AQ with CT-DNA were found to be 2.4157×10^6 L mol^{-1} and 1.25×10^6 M^{-1}, respectively. These values were compared with Stern−Volmer quenching constant of 2-aminoanthraquinone with CT-DNA which was 1.246×10^3 L mol^{-1} demonstrating that compound have strong binding affinity toward CT-DNA.[43] The Stern−Volmer quenching constant of DO3A-Act-AQ was found to be higher than reported for other macrocyclic moiety like 1,4,7-triazacyclononane (TACN, 0.053 ± 0.010).[44] CD spectrum of CT-DNA exhibits a positive absorption band at 282 nm due to the base stacking and a negative absorption band at 240 nm due to the helicity of B-DNA. The intensity of both bands decreased in the presence of DO3A-Act-AQ (1:1, CT-DNA-DO3A-Act-AQ) signifying unwinding of the double helix DNA after binding with the conjugate, leading to disturbing the secondary structure of DNA. Results obtained from fluorescence and CD spectroscopic studies concluded that compound strongly binds to DNA.[45] To increase the therapeutic potential of DO3A-Act-AQ, it can be complexed with β-emitting radionuclides; thus its complexation behavior with ^{153}Sm(III) and ^{177}Lu(III) was studied.[46] The essential requirement for DO3A-Act-AQ to be suitable for therapeutic purpose is the stable complex formation with metal ions along with the cytotoxicity toward cancer cells. A highly stable and strong complex formation was observed with both samarium and lutetium as found by high log K values obtained after titration, suggesting that the probe can be used with therapeutic metals for the treatment of cancer.

CONCLUSIONS

In conclusion, the synthetic strategy presented here demonstrates a facile way for the design of a macrocyclic ligand with DNA binding ligand like anthraquinone. The significant tumor targeting property makes it a candidate of choice for PET imaging. The cytotoxicity, induction of apoptosis in cancer cells, formation of highly stable complex with therapeutic metals like samarium and lutetium and preferential strong binding with CT-DNA can be used to understand the mechanism of anticancer nature and further expands its application from diagnosis to therapy.

ASSOCIATED CONTENT

Supporting Information

^{1}H, ^{13}C NMR, high resolution mass spectra and HPLC profiles of *tert*-butyl 2,2′,2″-(1,4,7,10-tetraazacyclododecane-1,4,7 triyl)-triacetate (**1**), 2-chloro-*N*-(9,10-dioxo-9,10-dihydroanthracen-

dx.doi.org/10.1021/mp4004089 | *Mol. Pharmaceutics* 2014, 11, 445−456

1-yl)acetamide (**2**), *tert*-butyl 2,2′,2″-(10-(2-(9,10-dioxo-9,10-dihydroanthracen-1-ylamino)-2-oxoethyl)-1,4,7,10-tetraazacyclododecane-1,4,7-triyl)triacetate (**3**), and 2,2′,2″-(10-(2-(9,10-dioxo-9,10-dihydroanthracen-1-ylamino)-2-oxoethyl)-1,4,7,10-tetraazacyclododecane-1,4,7-triyl)triacetic acid (**4**). The human serum stability curve, absorption, fluorescence, and CD spectra at 298 K, protonation constant, and stability constant of DO3A-Act-AQ with Cu(II), Ga(III), Sm(III), and Lu(III). This material is available free of charge via the Internet at http://pubs.acs.org.

AUTHOR INFORMATION

Corresponding Authors

*Tel.: +91-11-23905123, 23905117. E-mail: anupama@inmas.drdo.in.

*E-mail: akmishra63@gmail.com.

Notes

The authors declare no competing financial interest.

ACKNOWLEDGMENTS

This work was made possible by a financial contribution from DRDO, project INM-311.3.1. We thank Dr. R. P. Tripathi, Director, Institute of Nuclear Medicine and Allied Sciences, Defence Research and Development Organization for providing excellent research facilities.

REFERENCES

(1) Danhier, F.; Breton, A. L.; Preat, V. RGD-based strategies to target alpha(v) Beta(3) integrin in cancer therapy and diagnosis. *Mol. Pharmaceutics* **2012**, *9*, 2961−2973.

(2) Mohan, P.; Rapoport, N. Doxorubicin as a molecular nanotheranostic agent: Effect of doxorubicin encapsulation in micelles or nanoemulsions on the ultrasound-mediated intracellular delivery and nuclear trafficking. *Mol. Pharmaceutics* **2010**, *7*, 1959−1973.

(3) Johnson, M. G.; Kiyokawa, H.; Tani, S.; Koyama, J.; Morris-Natschke, S. L.; Mauger, A.; Bowers-Daines, M. M.; Lange, B. C.; Lee, K. H. Antitumor Agents 167. Synthesis and structure-activity correlations of the cytotoxic anthraquinone 1,4-Bis-(2,3-Epoxypropylamino)-9,10-anthracenedione and of related compounds. *Bioorg. Med. Chem.* **1997**, *5*, 1469−1479.

(4) Jones, J. E.; Amoroso, A. J.; Dorin, I. M.; Parigi, G.; Ward, B. D.; Buurma, N. J.; Pope, S. J. A. Bimodal, dimetallic lanthanide complexes that bind to DNA: the nature of binding and its influence on water relaxivity. *Chem. Commun.* **2011**, *47*, 3374−3376.

(5) Balasingham, R. G.; Williams, C. F.; Mottram, H. J.; Coogan, M. P.; Pope, S. J. A. Gold (I) complexes derived from Alkynoxy-substituted anthraquinones: syntheses, luminescence, cytotoxicity and cell imaging studies. *Organometallics* **2012**, *31*, 5835−5843.

(6) Huang, H. S.; Chiou, J. F.; Fong, Y.; Hou, C. C.; Lu, Y. C.; Wang, J. Y.; Shih, J. W.; Pan, Y. R.; Jeng, W. R.; Lin, J. J. Activation of human telomerase reverse transcriptase expression by some new symmetrical bis-substituted derivatives of the anthraquinone. *J. Med. Chem.* **2003**, *46*, 3300−3307.

(7) Jackson, T. C.; Verrier, J. D.; Kochanek, P. M. Anthraquinone-2-sulfonic acid (AQ2S) is a novel neurotherapeutic agent. *Cell Death Dis.* **2013**, *4*, 1−24.

(8) Teissier, E. M.; Bernier, J. L.; Lohez, M.; Catteau, J. P.; Henichart, J. P. Free radical production and DNA cleavage by copper chelating peptide-anthraquinones. *Anti Cancer Drug Des.* **1990**, *5*, 291.

(9) Teissier, E. M.; Boitte, N.; Helbecque, N.; Bernier, J. L.; Pommery, N.; Duvalet, J. L.; Fournier, C.; Hecquet, B.; Catteau, J. P.; Henichart, J. P. Synthesis and antitumor properties of an anthraquinone bisubstituted by the copper chelating peptide Gly-Gly-L-His. *J. Med. Chem.* **1993**, *36*, 2084.

(10) Meikle, I.; Cummings, J.; Macpherson, J. S.; Smyth, J. F. Identification of anthracenyl-dipeptide conjugates as novel topoisomerase I and II inhibitors and their evaluation as potential anticancer drugs. *Anti Cancer Drug Des.* **1995**, *10*, 515.

(11) Gatto, B.; Zagotto, G.; Sissi, C.; Cera, C.; Uriarte, E.; Palu, G.; Capranico, G.; Palumbo, M. Peptidyl anthraquinones as potential antineoplastic drugs: synthesis, DNA binding, redox cycling, and biological activity. *J. Med. Chem.* **1996**, *39*, 3114.

(12) Zagotto, G.; Sissi, C.; Gatto, B.; Palumbo, M. Aminoacyl-analogues of mitoxantrone as novel DNA-damaging cytotoxic agents. *Arkivoc* **2004**, *5*, 204.

(13) Teng, C. H.; Won, S. J.; Lin, C. N. Design. Synthesis and cytotoxic effect of hydroxyl- and 3-alkylaminopropoxy-9,10-anthraquinone derivatives. *Bioorg. Med. Chem.* **2005**, *13*, 3439−3445.

(14) Tu, H. Y.; Huang, A. M.; Teng, C. H.; Hour, T. C.; Yang, S. C.; Pu, Y. S.; Lin, C. N. Anthraquinone derivatives induce G_2/M cell cycle arrest and apoptosis in NTUB1 cells. *Bioorg. Med. Chem.* **2011**, *19*, 5670−5678.

(15) Huang, H. S.; Chiu, H. F.; Lee, A. R.; Guo, C. L.; Yuan, C. L. Synthesis and structure-activity correlations of the cytotoxic bifunctional 1,4-diamidoanthraquinone derivatives. *Bioorg. Med. Chem.* **2004**, *12*, 6163−6170.

(16) Wadas, T. J.; Wong, E. H.; Weisman, G. R.; Anderson, C. J. Coordinating radiometals of copper, gallium, indium, yttrium and zirconium for PET and SPECT imaging of disease. *J. Chem. Rev.* **2010**, *110*, 2858−2902.

(17) Bartholoma, M. D.; Louie, A. S.; Valliant, J. F.; Zubieta, J. Technetium and gallium derived radiopharmaceuticals: comparing and contrasting the chemistry of two important radiometals for the molecular imaging era. *J. Chem. Rev.* **2010**, *110*, 2903−2920.

(18) Benetollo, F.; Bombieri, G.; Calabi, L.; Aime, S.; Botta, M. Structural variations across the lanthanide series of macrocyclic DOTA complexes: insights into the design of contrast agents for Magnetic Resonance Imaging. *Inorg. Chem.* **2003**, *42*, 148−157.

(19) Tanwar, J.; Datta, A.; Tiwari, A. K.; Chaturvedi, S.; Ojha, H.; Allard, M.; Chaudary, N. K.; Thirumal, M.; Mishra, A. K. Facile synthesis of non-ionic dimeric molecular resonance imaging contrast agent: its relaxation and luminescence studies. *Dalton Trans.* **2011**, *40*, 3346−3351.

(20) Antunes, P.; Ginj, M.; Walter, M. A.; Chen, J.; Reubi, J. C.; Maecke, H. R. Influence of different spacers on the biological profile of a DOTA-somatostatin analogue. *Bioconjugate Chem.* **2007**, *18*, 84−92.

(21) Adhikari, M.; Dhaker, A.; Adhikari, J.; Ivanov, V.; Singh, V.; Chawla, R.; Kumar, R.; Sharma, R.; Karamalakova, Y.; Gadjeva, V.; Arora, R. In vitro studies on radioprotective efficacy of silymarin against γ-irradiation. *Int. J. Radiat. Biol.* **2013**, *89*, 200−211.

(22) Tanwar, J.; Datta, A.; Tiwari, A. K.; Thirumal, M.; Chuttani, K.; Mishra, A. K. Preclinical evaluation of DO3P-AME-DO3P: A polyazamacrocyclic methylene phosphonate for diagnosis and therapy of skeletal metastases. *Bioconjugate Chem.* **2011**, *22*, 244−255.

(23) Zagotto, G.; Ricci, A.; Vasquez, E.; Sandoli, A.; Benedetti, S.; Palumbo, M.; Sissi, C. Tuning G-quadruplex vs double-stranded DNA recognition in regioisomeric lysyl-peptidyl-anthraquinone Conjugates. *Bioconjugate Chem.* **2011**, *22*, 2126−2135.

(24) Huang, H.; Huang, K.; Li, C.; Huang, Y.; Chiang, Y.; Huang, F.; Lin, J. Synthesis, human telomerase inhibition and anti-proliferative studies of a series of 2,7-bis-substituted amido-anthraquinone derivatives. *Bioorg. Med. Chem.* **2008**, *16*, 6976−6986.

(25) Hoigebazar, L.; Jeong, J. M.; Hong, M. K.; Kim, Y. J.; Lee, J. Y.; Shetty, D.; Lee, Y. S.; Lee, D. S.; Chung, J. K.; Lee, M. C. Synthesis of ^{68}Ga-labeled DOTA-nitroimidazole derivatives and their feasibilities as hypoxia imaging PET tracers. *Bioorg. Med. Chem.* **2011**, *19*, 2176−2181.

(26) Velikyan, I.; Beyer, G. J.; Langstrom, B. Microwave-supported preparation of ^{68}Ga bioconjugates with high specific radioactivity. *Bioconjugate Chem.* **2004**, *15*, 554−560.

(27) Lacerda, S.; Campello, M. P.; Marques, F.; Gano, L.; Kubicek, V.; Fouskov, P.; Toth, E.; Santos, I. A novel tetraazamacrocycle bearing a thiol pendant arm for labeling biomolecules with radiolanthanides. *Dalton Trans.* **2009**, *23*, 4509−4518.

(28) Riss, P. J.; Burchardt, C.; Roesch, F. A methodical ^{68}Ga-labelling study of DO2A-(butyl-L-tyrosine)$_2$ with cation-exchanger post-processed ^{68}Ga: practical aspects of radiolabelling. *Contrast Media Mol. Imaging* **2011**, *6*, 492−498.
(29) Chakravarty, R.; Chakraborty, S.; Dash, A.; Pillai, M. R. A. Detailed evaluation on the effect of metal ion impurities on complexation of generator eluted ^{68}Ga with different bifunctional chelators. *Nucl. Med. Biol.* **2013**, *40*, 197−205.
(30) Fani, M.; Andre, J. P.; Macke, H. R. ^{68}Ga-PET: A powerful generator-based alternative to cyclotron based PET radiopharmaceuticals. *Contrast Media Mol. Imaging* **2008**, *3*, 67−77.
(31) Tietze, L. F.; Gericke, K. M.; Schuberth, I. Synthesis of highly functionalized anthraquinones and evaluation of their antitumor activity. *Eur. J. Org. Chem.* **2007**, 4563−4577.
(32) Wang, S.; Wang, Q.; Wang, Y.; Liu, L.; Weng, X.; Li, G.; Zhang, X.; Zhou, X. Novel anthraquinone derivatives: Synthesis via click chemistry approach and their induction of apoptosis in BGC gastric cancer cells via reactive oxygen species (ROS)-dependent mitochondrial pathway. *Bioorg. Med. Chem. Lett.* **2008**, *18*, 6505−6508.
(33) Huang, H.; Chiou, J.; Fong, Y.; Hou, C.; Lu, Y.; Wang, J.; Shih, J.; Pan, Y.; Lin, J. Activation of human telomerase reverse transcriptase expression by some new symmetrical bis-substituted derivatives of the anthraquinone. *J. Med. Chem.* **2003**, *46*, 3300−3307.
(34) Zagotto, G.; Sissi, C.; Lucatello, L.; Pivetta, C.; Cadamuro, S. A.; Fox, K. R.; Neidle, S.; Palumbo, M. Aminoacyl-anthraquinone conjugates as telomerase inhibitors: Synthesis, biophysical and biological evaluation. *J. Med. Chem.* **2008**, *51*, 5566−5574.
(35) Huang, H.; Chiu, H.; Lee, A.; Guo, C.; Yuana, C. Synthesis and structure−activity correlations of the cytotoxic bifunctional 1,4-diamidoanthraquinone derivatives. *Bioorg. Med. Chem.* **2004**, *12*, 6163−6170.
(36) Breeman, W. A.; Blois, E.; Chan, H. S.; Konijnenberg, M.; Kwekkeboom, D. J.; Krenning, E. P. ^{68}Ga-labeled DOTA-Peptides and ^{68}Ga-labeled Radiopharmaceuticals for Positron Emission Tomography: Current Status of Research, Clinical Applications, and Future Perspectives. *Semin. Nucl. Med.* **2011**, *41*, 314−321.
(37) Hua, F.; Cutlerb, C. S.; Hoffmanc, T.; Sieckmanc, G.; Volkertc, W. A.; Jurisson, S. S. Pm-149 DOTA bombesin analogs for potential radiotherapy: In vivo comparison with Sm-153 and Lu-177 labeled DO3A-amide-Ala-BBN(7−14)NH2. *Nucl. Med. Biol.* **2002**, *29*, 423−430.
(38) Costantini, D. L.; Villani, D. F.; Vallis, K. A.; Reilly, R. M. Methotrexate, Paclitaxel, and Doxorubicin Radiosensitize HER2-Amplified Human Breast Cancer Cells to the Auger Electron−Emitting Radiotherapeutic Agent ^{111}In-NLS-Trastuzumab. *J. Nucl. Med.* **2010**, *51*, 477−483.
(39) Viola-Villegas, N.; Vortherms, A.; Doyle, R. P. Targeting Gallium to Cancer Cells through the Folate Receptor, Drug. *Target Insights* **2008**, *3*, 13−25.
(40) Wang, S.; Wang, Q.; Wang, Y.; Liu, L.; Weng, X.; Li, G. Novel anthraquinone derivatives: synthesis via click chemistry approach and their induction of apoptosis in BGC gastric cancer cells via reactive oxygen species (ROS)-dependent mitochondrial pathway. *Bioorg. Med. Chem. Lett.* **2008**, *18*, 6505−6508.
(41) Tua, H.; Huangb, A.; Tenga, C.; Hourb, T.; Yanga, S.; Puc, Y.; Lin, C. Anthraquinone derivatives induce G_2/M cell cycle arrest and apoptosis in NTUB1 cells. *Bioorg. Med. Chem.* **2011**, *19*, 5670−5678.
(42) Lepecq, J. B.; Paoletti, C. A fluorescent complex between ethidium bromide and nucleic acids: Physical-Chemical characterization. *J. Mol. Biol.* **1967**, *27*, 87−106.
(43) Yang, H.; Song, W.; Jing, M.; Liu, R. Study on the interaction mechanism of 2-aminoanthraquinone with calf thymus DNA. *J. Biochem Mol. Toxicology* **2013**, *27*, 272.
(44) Xu, W.; Yang, X.; Yang, L.; Jia, Z.; Liu, F.; Lu, G. Synthesis and DNA cleavage activity of triazacrown-anthraquinone conjugates. *New J. Chem.* **2010**, *34*, 2654−2661.
(45) Sheng, X.; Guo, X.; Lu, X.; Lu, G.; Shao, Y.; Liu, F.; Xu, Q. DNA Binding, Cleavage, and Cytotoxic Activity of the Preorganized dinuclear zinc(II) complex of Triazacyclononane derivatives. *Bioconjugate Chem.* **2008**, *19*, 490−498.
(46) Cutler, C. S.; Hennkens, H. M.; Sisay, N.; Huclier-Markai, S.; Jurisson, S. S. Radiometals for combined imaging and therapy. *Chem. Rev.* **2013**, *113*, 858−883.